GEOLOGIJA. 2008. No. 1(61). P. 1–16

Petrology • Petrologija • Петрология

Extensive charnockitic-granitic magmatism in the crystalline crust of West Lithuania

Gediminas Motuza,

Vykintas Motuza,

Ekaterina Salnikova,

Aleksandr Kotov

Motuza G., Motuza V., Salnikova E., Kotov A. Extensive charnockitic-granitic magmatism in the crystalline crust of West Lithuania. *Geologija*. Vilnius. 2008. No. 1(61). P 1–16. ISSN 1392-110X

A number of plutons of charnockitic and granitic rocks have been revealed in the West Lithuanian Granulite Domain in the course of the recent geological mapping. The largest, Kuršiai (Curonian), batholith has been identified by gravity and magnetic anomalies and drill cores of 86 wells. Intrusions are composed of rocks of intermediate to felsic composition systematically attributed to charnockite, enderbite, mangerite, opdalite and granite. Rocks, characterized by 53 new ICP-MS and ES analyses, combine geochemical patterns characteristic both of A and S type granites being predominantly ferroan, alkali-calcic and calc-alkaline, high potassic to shoshonitic, but at the same time mainly peraluminous. Four U–Pb ID-TIMS zircon dates suggest formation of a charnockitic-granitic suite at around 1.85–1.82 Ga, presumably in the transitional period from the late orogenic to cratonic stages of formation of the continental crust.

Key words: charnockite, granite, geochemistry, radiological dating, magmatism

Received 06 November 2007, accepted 18 January 2008

Gediminas Motuza, **Vykintas Motuza**. Department of Geology and Mineralogy, Vilnius University, M. K. Čiurlionio 21/27, LT-03101 Vilnius, Lithuania. E-mail: gediminas.motuza@gf.vu.lt. **Ekaterina Salnikova**, **Aleksander Kotov**. Institute of Precambrian Geology and Geochronology, emb. Adm. Makarov 2, Sankt Petersburg, Russia

INTRODUCTION

The western part of Lithuania is situated near the western margin of East European Craton in the Svekofennian domain. The crystalline crust is covered by Phanerozoic sediments, and information on its composition and structure has been acquired by drilling and geophysical methods. Drill cores of about 200 wells are available from this part of the country, stored in the Central Drill Core Storage of the Geological Survey of Lithuania.

A large polyphase Kuršiai (Curonian) charnockitic batholith, along with a few smaller charnockitic and granitic plutons, has been revealed by recent geological mapping of the crystalline basement, performed on behalf of the Geological Survey of Lithuania. In original industrial drilling reports and publications by previous researchers, these rocks where considered to be gabbros and diorites altered metasomatically, granites or charnockitic migmatites of unknown age and body shape (R. Gailius in Lietuvos geologija, 1994; Stirpeika, 1999). The current paper presents results from a recent revision and reinterpretation of available drill core and thin sections, as well as new geochemical data and U–Pb ID-TIMS zircon dating results characterizing the composition of the discovered charnockitic plutons. Together with coeval granitic plutons they do mark a particular phase of extensive plutonic magmatism in this region, presumably related to later phases of Svekofennian orogeny.

GEOLOGICAL SETTING

The spread of charnockitic and granitic plutons under consideration is limited to the West Lithuanian Granulite Domain (WLGD) regarded as a particular lithospheric block with a composition and structure distinct from adjacent domains (Fig. 1).

The general thickness of the crust in the WLGD is comparatively low (40–45 km), with the upper crust being thick (30 km) and the lower crust thin (10 km). In adjacent domains – East Lithuania to the east and Västervik-Gotland to the west – the crust is thicker (50–55 km) and more variable both in terms of thickness and composition (Eurobridge'95 seismic working group, 2001; Giese, 1998; Bogdanova et al., 2006; Motuza, 2005a, b). This may reflect a higher degree of denudation of the crystalline crust in the WLGD and exposure of more deeply originated lithological assemblages on its recent surface.

In terms of metamorphism, the WLGD is a high-grade terrain. Remnants of supracrustals are metamorphosed under conditions of granulite facies, highly migmatized and preserved in fragments of bodies in small areas, while predominant lithologies in the crystalline basement are diatexitic migmatites and plutonic rocks (Fig. 1).

Supracrustals are represented by calcium-rich gneisses – primary greywackes formed by local redeposition of weakly sorted volcanic material, metapelitic gneisses formed mainly

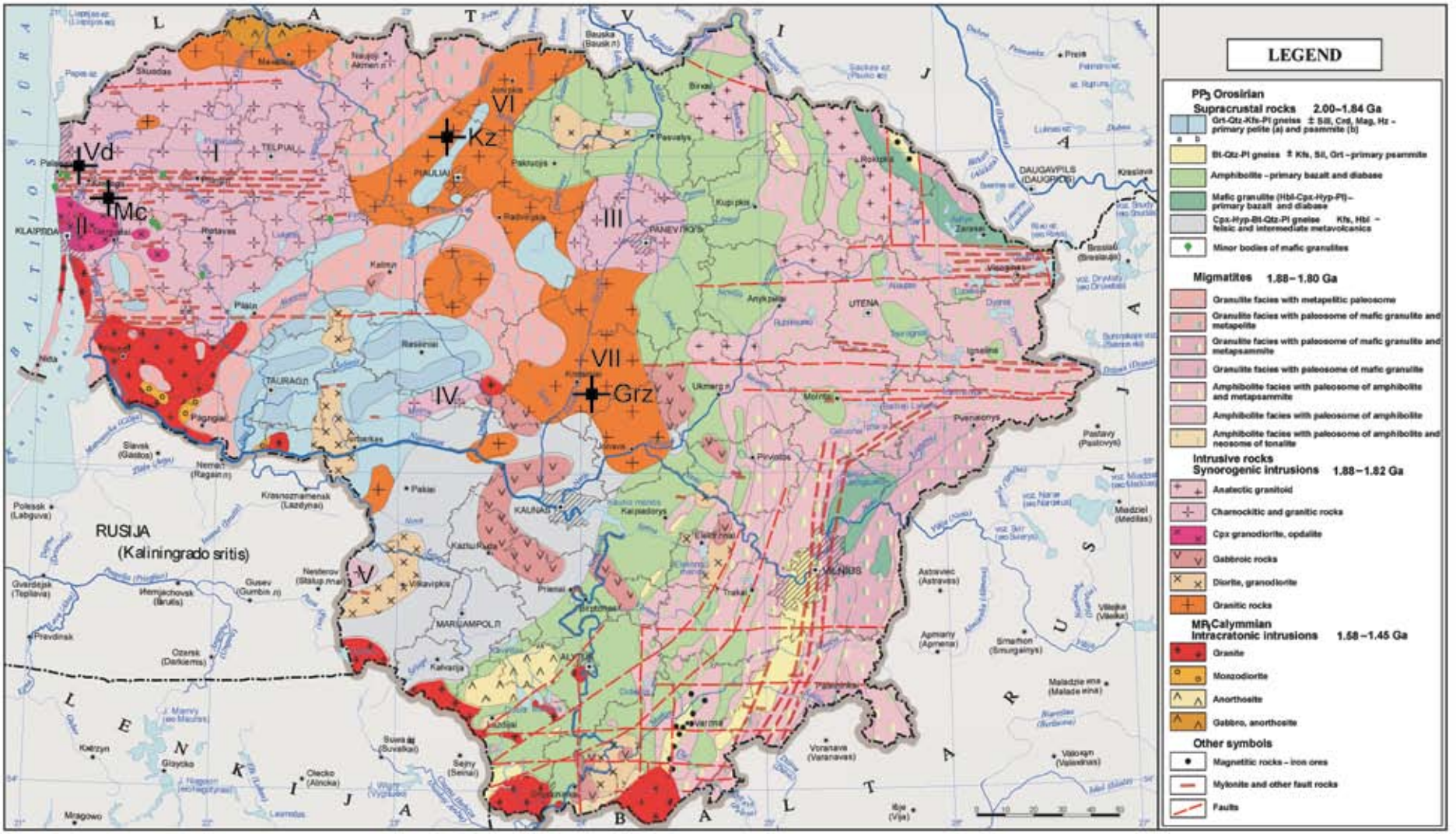

Fig. 1. Geological map of the crystalline basement of Lithuania, compiled by G. Motuza, computer design by R. Svilienė
Numbers indicate plutons: I – Kuršiai, II – Pilsotas phase of Kuršiai pluton, III – Sidabravas; IV – Ariogala, V – Kybartai, VI – Kužiai, VII – Kėdainiai.
Crosses mark position of samples for U–Pb dating: Mc – Macuičiai, Kz – Kužiai, Grz – Graužai, Vd – Vydmantai

Fig. 1. Lietuvos kristalinio pamato žemėlapis (sudarė G. Motuza, kompiuterinis apipavidalinimas R. Svilienės).
Numeriais pažymėti plutonai: I – Kuršių; II – Kuršių plutono Pilsoto fazė; III – Sidabravo; IV – Ariogalos; V – Kybartų; VI – Kužių, VII – Kėdainių.
Kryželiais pažymėtos U–Pb metodu datuotų pavyzdžių vietos: Mc – Macuičiai; Kz – Kužiai; Grz – Graužai; Vd – Vydmantai

from the same source rocks as calcium-rich gneisses, but more weathered, felsic gneisses and quartzite – metamorphosed mature arcositic sandstones. Supracrustals where formed in the tectonic environment transitional from a volcanic island arc to an active continental margin. Mafic supracrustals are not known in the WLGD on the recent surface of the crystalline crust.

The possible age of sedimentation is limited by an interval of 2.0–1.85 Ga. The former figure is the age of the youngest detrital zircon in migmatized metapelite (Skridlaite et al., 2007a). The later figure is based on the age of oldest dated intrusive rocks, which are charnockites (Motuza, 2005a, b).

There are at least three generations of plutonic rocks in the WLGD. To the oldest generation, emplaced at 1.85–1.815 Ga, belong the charnockitic and granitic plutons under consideration. The Riga AMCG pluton might be attributed to the second generation formed at 1.58 Ga (Rämo et al., 1996), along with intrusions of the Mazury belt in Poland, including Veisiejai and Kabeliai in Lithuania, formed between 1.56–1.5 Ga (Dörr et al., 2002; Sundblad et al., 1994). To the youngest generation belong plutons of granites with minor phases of quartz monzodiorites formed around 1.46 Ga (Motuza et al., 2006; Skridlaitė et al., 2007b).

The WLGD is separated from the East-Lithuanian domain by a roughly N–S trending Mid-Lithuanian Suture Zone (MLSZ). It is this zone of rapid lateral changes of crustal structure where the Mocho gradually deepens from 40 to 50 km (Eurobridge'95 seismic working group, 2001). It is also marked by a specific rock assemblage forming two parallel belts. The eastern belt is composed predominantly of amphibolites (metabasalts and metadiabases) and subordinated metasedimentary rocks, while the western belt consists of metavolcanics of andesitic-dacitic composition (Motuza, 2005a, b).

The western interface of the WLGD, with the Västervik-Gotland crustal block, is less clear, distinguished mainly by a gradual deepening of the Mocho, as revealed on the Eurobridge DSS profile in the central part of the Baltic Sea (Giese, 1998).

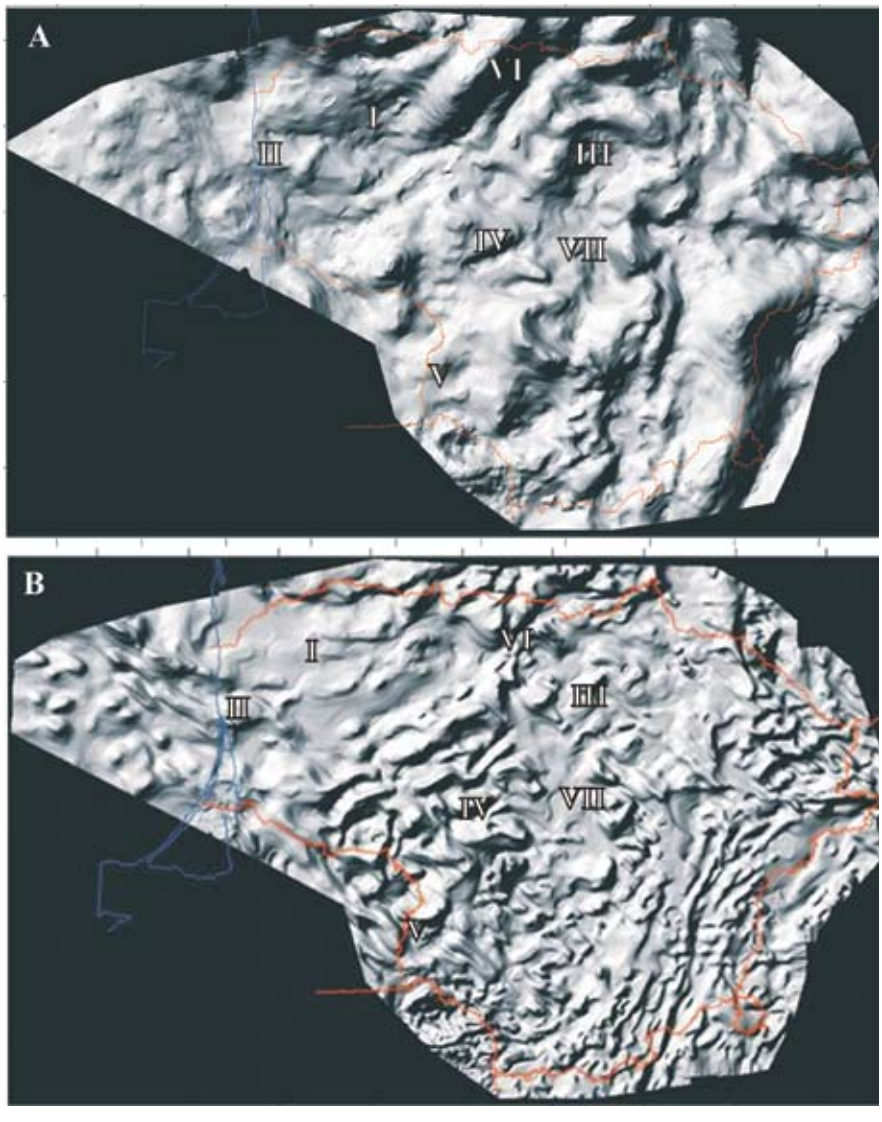

Fig. 2. Relief-shaded gravity (*A*) and magnetic (*B*) anomaly maps of Lithuania. Compiled by L. Korabliova, Geological Survey of Lithuania. Numbers indicate charnockitic and granitic plutons as in Fig. 1

Fig. 2. Lietuvos gravitacinių (*A*) ir magnetinių (*B*) anomalijų reljefinis šešėlinis žemėlapis (sudarė L. Korabliova, Lietuvos geologijos tarnyba.). Čarnokitų ir granitų plutonų numeracija kaip 1 pav.

GEOLOGICAL POSITION OF CHARNOCKITIC-GRANITIC PLUTONS

The charnockitic and granitic rocks of the oldest generation of intrusive rocks form the Kuršiai (Curonian) batholith and a few smaller bodies (Fig. 1). The Kuršiai batholith is regarded to encompass an area of approximately 140×80 km in northwestern Lithuania, extending offshore into the Baltic Sea. The batholith is almost entirely composed of charnockitic rocks, except for a few small enclaves of migmatized supracrustals and minor bodies of granites. Charnockitic rocks by cores obtained from 86 drill holes were confirmed. Most of the drill holes are regularly spaced over the area of the batholith, but some of them are concentrated in oil fields in the Telšiai fault zone.

The area of the Kuršiai batholith is distinguished by extended gravity and magnetic lows are not uniform in nature, thus reflecting a variation of lithology and shape of the body (Fig. 2).

Along with the largest Kuršiai batholith in the WLGD, a few smaller charnockiticplutons – Sidabravas, Ariogala and Kybartai – were revealed. They are distinguished by potential field anomalies and characterized just by a single drill hole each – Kurtuvėnai-166, Pramėdžiuva-97 and Kybartai-39, respectively (Figs. 1, 2).

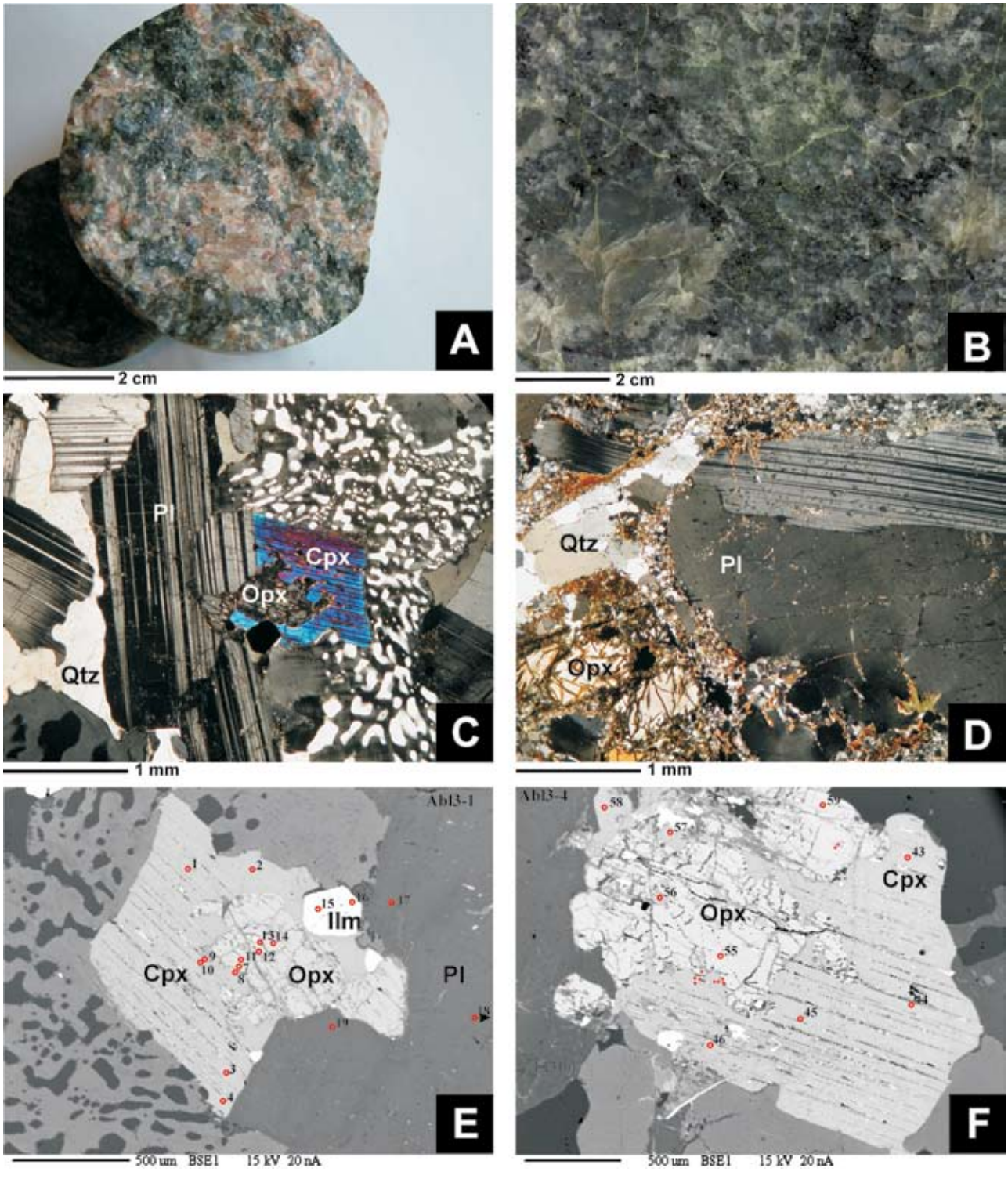

Fig. 3. Charnockites in hand specimens from wells Stumbres (*A*) and Macuičiai (*B*); in thin sections from wells Ablinga-3 (*C*) and Eitučiai (*D*); in SEM microphotographs of thin section from well Ablinga-3, (*E, F*), the same as in *C*

Fig. 3. Čarnokitų kerno nuotraukos iš Stumbrių (*A*) ir Macuičių (*B*) gręžinių; šlifų nuotraukos iš Ablingos-3 (*C*) ir Eitučių (*D*) gręžinių; nuskaitančio mikroskopo nuotraukos iš Ablingos-3 gręžinio šlifo (*E, F*), to paties kaip ir *C*

PETROGRAPHIC FEATURES

The mineralogical and structural characteristic of rocks is based on examination of numerous thin sections supported by SEM microprobe studies carried out at the Geological Department of Warsaw University.

Typical rock-forming minerals are plagioclase (No. 40–55), K-feldspar, quartz, hypersthene, biotite, clinopyroxene, garnet which forms up to 20% of the rock but is not always present. The bulk content of mafic minerals is mainly 20–30% (Fig. 3).

Usual accessory minerals are magnetite, ilmenite, herzinite, zircon, monazite, xenotime, and fluorapatite. Hornblende is present in a few places as a secondary mineral forming substitution rims in clinopyroxene.

The mineralogical composition shows that the Kuršiai batholith and other plutons are composed by various types of rocks – charnockite, enderbite, opdalite, mangerite, jotunite. Such variation is reflected also in the accompanying diagram based on the normative content of felsic minerals (Fig. 4).

In the western part of the Kuršiai pluton, there appear three minor bodies composed by clinopyroxene granodiorite and, in places, opdalite containing hypersthene (Fig. 1). In this area, rocks are more uniform in terms of mineralogical and geochemical composition. They are distinguished also by a higher magnetic susceptibility. Presumably, these rocks where formed by a particular magmatic pulse and are regarded as a distinct Pilsotas phase.

The texture of charnockitic rocks is characteristic of intrusive rocks. In all varieties it is middle- (1–5 mm) to coarse-grained (5–10 mm), often porphyry formed by K-feldspar and plagioclase phenocrysts up to 20–30 mm in diameter. Plagioclase is often euhedral or hypidiomorphic with simple twins and oscillatory zoning. In places, a granophyric texture is well developed (Fig. 3, c). Hypersthene appears mainly in separate grains, in places overgrown by clynopyroxene, indicating an earlier crystallization of orthopyroxene and its magmatic origin (Fig. 3e, f). The primary structure is massive, but in places, particularly in the Telšiai Shear Zone, rocks are deformed to different degree (Fig. 3d) and transformed to high-grade mylonites (Motuza, Vėjelytė, 2005 and figures therein).

GEOCHEMICAL CHARACTERISTIC

Charnockitic rocks

The geochemical characteristic of charnockitic rocks is based on 50 samples which have been analyzed at the Acme Analytical Laboratories Ldt., Canada. For the main elements and Ba, Cr, Sc ICP-ES, as well as for other trace elements ICP-MS spectrometry was applied. Samples represent principal varieties of rocks in particular wells, with the aim to characterize the geochemical variation in the whole area rather than in particular sections. The Kuršiai pluton is characterized by 47 analyses, while the other charnockitic plutons by just three analyses. Two of them are from Sidabravas (Kur-166) and one from Ariogala pluton (Prmd-97). The analytical results are listed in Table 1.

SiO_2 content in charnockitic rocks varies from 53 to 73 and in average is 63% (Fig. 4).

Harker diagrams demonstrate a regular distribution and a good correlation of FeO, MgO, TiO_2, CaO, P_2O_5, V, Co, Sr, versus SiO_2. Other elements (Al_2O_3, K_2O, MnO, Cr_2O_3, Sc, Nb, Rb, Ga, REE, Na_2O, Ba) show a weak or no correlation with SiO_2 (Fig. 5).

Such compositional variation reflects the variety of rocks in different places of the Kuršiai pluton presumably formed during particular phases of pluton formation.

Applying principles of granitoid classification by Frost et al. (2001), all charnockitic rocks were attributed to the ferroan type (Fig. 6).

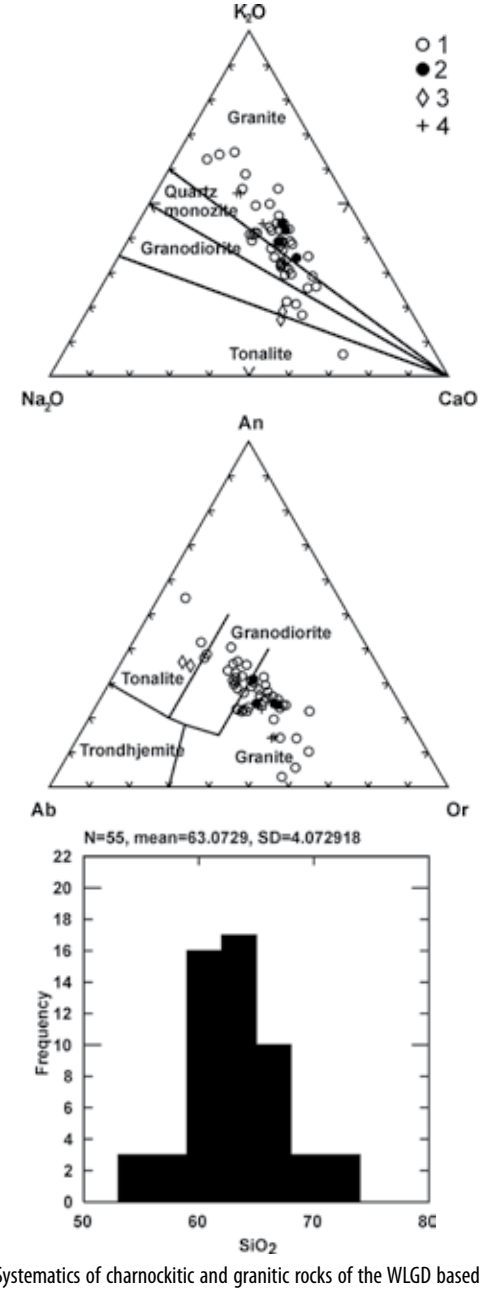

Fig. 4. Systematics of charnockitic and granitic rocks of the WLGD based on Na_2O–K_2O–CaO triplot by Rajesh and Santosh (2004); normative ternary diagram by Barker (1979) and histogram of SiO_2 content. Symbols: *1* – charnockitic rocks of Kuršiai pluton, *2* – rocks of Pilsotas phase of Kuršiai pluton, *3* – charnockitic rocks of Sidabravas and Ariogala plutons, *4* – granites of Kužiai, Ledai and Kėdainiai plutons

Fig. 4. VLGD čarnokitų ir granitų suskirstymas remiantis Na_2O–K_2O–CaO trikampe diagrama (pagal Rajesh and Santosh, 2004); Norminių Ab–An–Or kiekių (pagal Barker, 1979) ir SiO_2 kiekio histograma. Sutartiniai ženklai: *1* – Kuršių plutono čarnokitai; *2* – Kuršių plutono Pilsoto fazės uolienos; *3* – Sidabravo ir Ariogalos plutonų čarnokitai; *4* – Kužių, Ledų ir Kėdainių plutonų granitai

According to the Modified Alkali-Lime Index (MALI), the rocks belong to alkali-calcic and calc-alkalic types (Fig. 6). They are also subalkaline, high-potassic to shoshonitic, except enderbite which is medium-potassic (Fig. 6).

In the discrimination diagrams by Whalen, most of samples are located in the A-type field or close to its limits (Whalen, 1987) (Fig. 6).

Using the criteria by Chappell and White (Chappell, White, 2001), most of the charnockitic rocks may be attributed to S-type granites (Fig. 7). The Alumina Saturation Index varies between 1.2 and 2.1, but on modified Shand's diagram (Maniar, Piccoli, 1989) part of rocks appear to be metaluminous, particularly those from the Pilsotas phase (Fig. 7). This is in agreement with the presence of modal garnet and normative corundum in rocks.

On the Nakamura chondrite-normalized REE abundance diagrams charnockitic rocks might be divided into three principal groups. The distribution of rocks included in different groups does not reveal any regularity in area, except group IV embracing rocks of the Pilsotas phase (Fig. 8):

Group I is characterized by a comparatively low content of REE and absence of any Eu anomaly. The chondrite-normalized La content varies between 120 and 200, and the La / Lu ratio is mainly around 30. It comprises about 20% of the sampled rocks.

Group II by a higher general content of REE and an evident, but moderately negative, Eu anomaly is characterized. It comprises about 70% of the total analysis. Based on the abundance of LREE, this group might be tentatively subdivided in two subgroups: II a – La content is around 100–200 and II b – La content varies between 200 and 400.

Group III is distinguished by a higher total content of REE, particularly LREE, a prominent negative Eu anomaly and quite uniform REE abundance patterns. These rocks are localized in the NW part of the Kuršiai batholith and belong to the Pilsotas phase of intrusion.

Analysis of the charnockitic rocks of the Sidabravas and Ariogala plutons are plotted on the same diagrams and distinguished by special symbols. The geochemical patterns of these rocks fit well with those of the Kuršiai pluton in general.

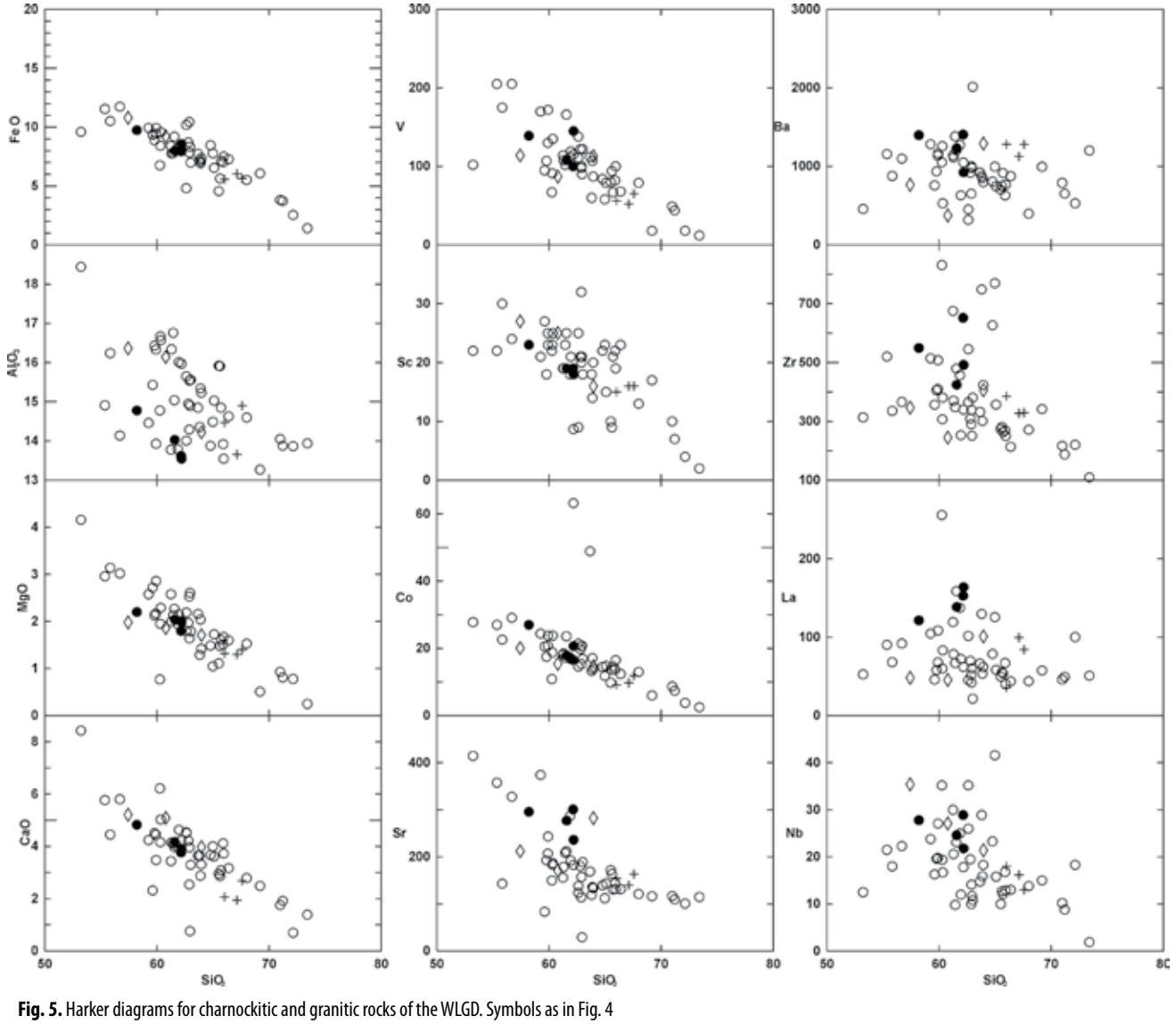

Fig. 5. Harker diagrams for charnockitic and granitic rocks of the WLGD. Symbols as in Fig. 4

Fig. 5. VLGS čarnokitų ir granitų Harkerio diagramos. Sutartiniai ženklai kaip 4 pav.

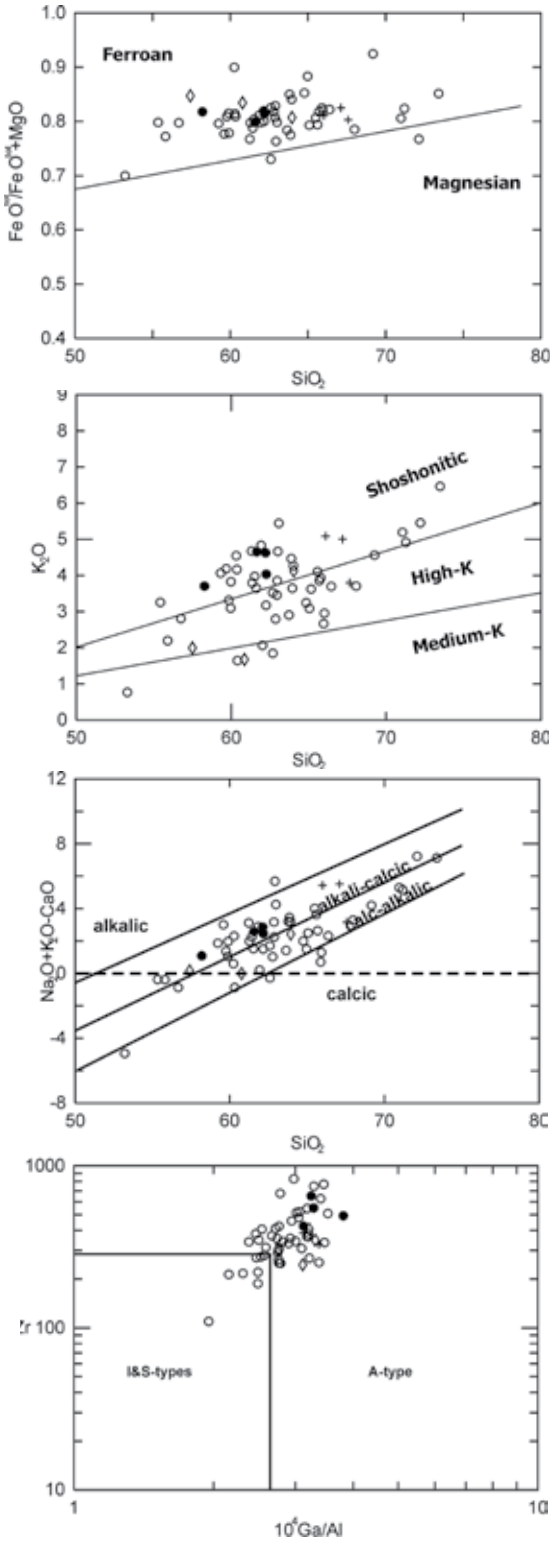

Fig. 6. Diagrams reflecting geochemical patterns of charnockitic and granitic rocks in the WLGD, characteristic of A-type granites: SiO_2 vs FeO^{tot} / FeO^{tot} + MgO diagram and SiO_2 *vs* $Na_2O + K_2O$–CaO (Modified Alkali-Lime Index) diagram, both by Frost et al. (2001); SiO_2 *vs* K_2O diagram by Peccerillo and Taylor (1976); 10^4Ga / Al *vs* Zr diagram by Whalen et al. (1987). Symbols as in Fig. 4

Fig. 6. VLGS čarnokitų ir granitų geocheminės sudėties diagramos, rodančios artimumą A tipo granitams: SiO_2 vs FeO^{tot} / FeO^{tot} + MgO ir SiO_2 *vs* $Na_2O + K_2O$–CaO (modifikuoto šarmingumo-kalcingumo rodiklio) (abi pagal Frost et al., 2001); SiO_2 *vs* K_2O (pagal Peccerillo and Taylor, 1976); 10^4Ga / Al *vs* Zr (pagal Whalen et al., 1987). Sutartiniai ženklai kaip 4 pav.

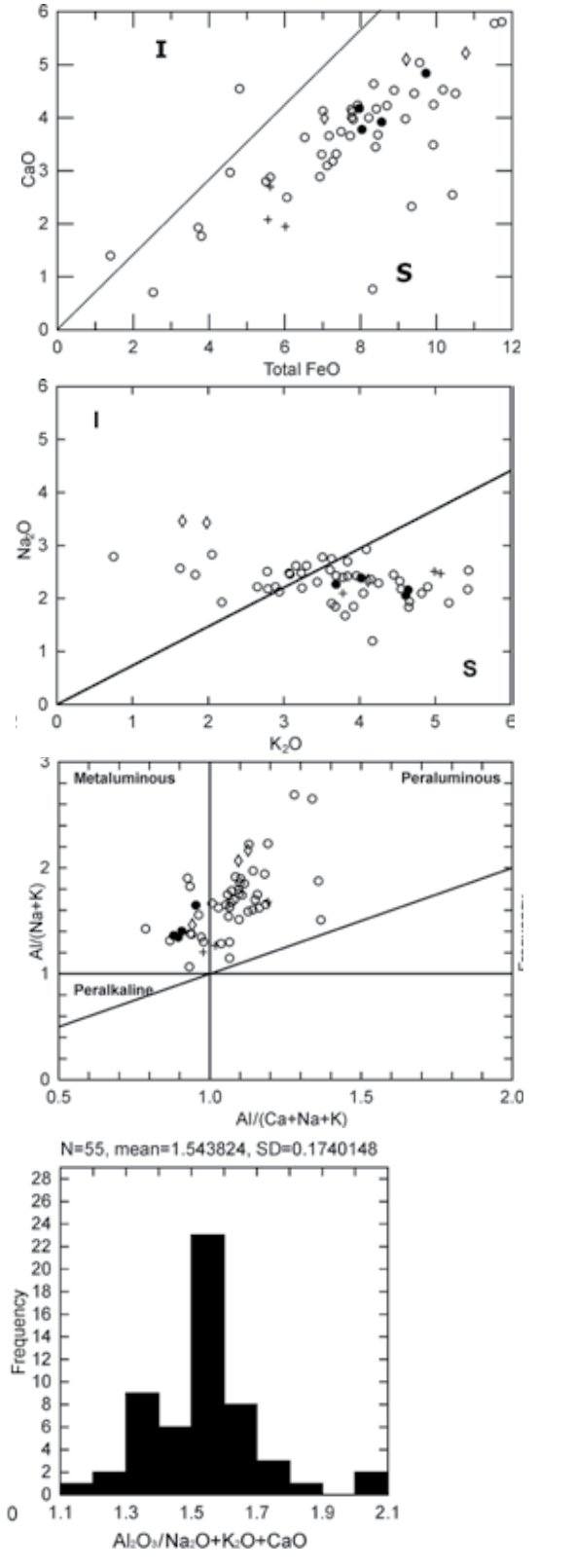

Fig. 7. Diagrams reflecting geochemical patterns of charnockitic and granitic rocks in WLGD characteristic of S-type granites: total FeO *vs* CaO diagram; Na_2O *vs* K_2O diagram by Chapel, White (2001); plot of Shand's index modified by Maniar and Piccoli (1989), aluminium saturation index (ASI) histogram. Symbols as in Fig. 4

Fig. 7. VLGS čarnokitų ir granitų geocheminės sudėties diagramos, rodančios artimumą S tipo granitams: FeO *vs* CaO ir Na_2O *vs* K_2O (pagal Chapel, White, 2001); Šando rodiklio diagrama (pakeista pagal Maniar and Piccoli, 1989), aliumingumo rodiklio histograma. Sutartiniai ženklai kaip 4 pav.

Table 1. **Chemical analyses of the investigated rocks (dimentions: oxides in (%), other elements in (ppm))**
1 lentelė. **Tirtų uolienų cheminės analizės duomenys (vienetai: oksidai (%), kiti elementai (ppm))**

ROCK	Charnockitic rocks of Kuršiai pluton																				
SAMPLE	Abl-1	Abl-3	Abl-3	Akm-71	Bbl-2	Bbl-4	D-1	Et-1	Gnc-3	Grk-4	Grn-1	Krt-3	Kul-1	Lz-1	Mcc-1	Mm-1-1	Mkl-1	Pjr-3	Plk	Plng-2	Sdr
SiO_2	65.9	55.36	56.69	64.77	71.21	70.99	63.01	62.62	65.71	59.61	59.92	61.87	73.41	65.09	61.95	60.3	62.8	61.55	63.95	66.39	69.19
Al_2O_3	13.92	14.91	14.14	13.88	13.88	14.05	15.56	14.01	14.85	15.43	13.93	13.79	13.94	15.03	16.01	16.67	14.95	15.04	15.23	14.63	13.27
FeO	7.02	11.55	11.74	8.47	3.73	3.81	6.99	10.19	7.13	9.36	9.93	8.23	1.41	6.54	8.36	8.43	8.71	9.2	7.37	7.28	6.07
MgO	1.51	2.96	3.02	1.49	0.81	0.93	1.79	2.19	1.61	2.72	2.86	1.94	0.25	1.73	2.15	1.95	1.97	2.27	1.42	1.6	0.51
CaO	4.12	5.77	5.8	3.67	1.92	1.76	3.3	4.52	3.09	2.32	3.48	3.99	1.39	3.62	4.63	4.16	4.22	3.97	3.31	3.17	2.49
Na_2O	2.22	2.2	2.18	2.48	2.22	1.92	2.17	2.45	1.85	1.2	1.68	2.1	2.11	2.54	2.83	2.36	2.51	1.91	2.29	1.85	2.18
K_2O	2.65	3.24	2.79	3.23	4.9	5.18	5.43	1.83	3.92	4.17	3.81	4.82	6.45	3.61	2.05	4.15	2.78	3.63	4.25	3.68	4.55
TiO_2	0.9	2.32	2.16	1.04	0.44	0.47	0.99	1.5	0.93	1.3	1.7	1.49	0.14	0.88	1.29	1.16	1.15	1.62	0.98	0.79	0.64
P_2O_5	0.12	0.79	0.72	0.27	0.22	0.14	0.06	0.3	0.19	0.24	0.69	0.59	0.06	0.22	0.1	0.42	0.18	0.26	0.2	0.18	0.16
MnO	0.09	0.12	0.12	0.1	0.05	0.06	0.08	0.11	0.12	0.1	0.06	0.1	0.01	0.06	0.09	0.11	0.11	0.11	0.1	0.16	0.08
Cr_2O_3	0.01	0.011	0.009	0.007	0.008	0.007	0.009	0.009	0.005	0.003	0.007	0.005	0.003	0.012	0.009	0.01	0.009	0.006	0.009	0.006	0.005
Ba	630	1157	1099	806	653	790.6	2014	452	915	758	1167	1272	1203	746.7	631	1257	917	1204	799.4	876.3	995.2
Sc	22	22	24	22	7	10	18	25	21	27	23	18	2	15	21	23	21	25	20	23	17
Co	13.7	27	29.1	14.5	7.4	8.7	16.9	21.4	14.7	20.6	23.8	17.3	2.5	14.8	16.8	18.8	19.8	23.6	13.9	12.4	6
Cs	0.5	0.8	0.8	1.8	3	1.5	1	0.9	0.8	0.8	5.2	4	0.8	1.2	0.9	0.3	0.4	0.7	2	0.7	0.7
Ga	23.7	24.2	23.8	25	18.3	17.2	20.3	23.6	21.7	23.9	26	21.5	14.4	21.8	28.6	24.4	24.5	24.3	22.3	16.7	21.1
Hf	8.7	14	9.9	17.3	5.3	7	10.7	14.3	8.3	10.9	14.1	14.1	3.4	9.9	8.1	8.4	8.8	13.4	12.4	5.9	10.5
Nb	16.8	21.5	22.3	23.3	8.8	10.2	10.8	26	12.1	16.3	27.1	25	1.9	15.8	12	19.4	19.5	23.1	18.3	13	15
Rb	109.7	119.3	111.7	140.4	230.3	215.8	222.8	78.1	171.7	129.4	205	214.1	230.2	157.1	61.5	131.7	89.9	127.3	169.6	147.8	163.7
Sn	2	2	2	< 1	1	2	2	1	0.9	0.9	3	2	1	1	3	1	< 1	1	2	1	2
Sr	144	357.7	327.8	139.5	109.7	116.9	188.9	138.2	130.6	83.5	243.1	286.6	114.9	143.7	192.2	183.7	180.4	211.9	133.6	131.1	116.5
Ta	1.7	1.2	1.3	1.1	0.6	0.5	0.8	1.4	0.4	0.9	1.3	1.7	0.1	0.6	0.9	1.1	1	1.2	1.3	0.7	0.6
Th	12.3	14.9	13.6	20.5	21.1	22.5	4	34	13.4	17.2	28.4	41.3	41	21.9	13.9	5	17.6	56	21.4	13.6	16.7
Tl	0.4	0.1	0.1	0.3	0.1	0.2	0.1	0.3	0.6	0.6	0.7	0.7	<.1	0.4	0.2	0.4	0.1	0.3	0.2	0.2	0.1
U	1.2	1.3	1	1.3	2.9	2.2	0.5	2.2	1.1	0.7	1.3	4.7	1.3	0.8	1.5	0.5	1.1	1	1.7	0.8	1.4
V	82	205	205	84	44	49	122	111	67	95	172	112	12	79	119	91	122	166	87	68	18
W	< 1	0.5	0.3	< .1	< .1	0.1	0.2	0.9	2	0.9	0.5	5	0.1	0.1	< 1	0.9	< .1	0.9	0.4	<.1	0.1
Zr	269.3	520.3	366	626.8	187.8	216.9	380.6	545.4	263.7	356.8	508.1	456.9	109.6	357.1	253.2	307.4	309.4	479.7	423.4	213.6	342
Y	17.4	57.5	56	62	42.1	43.1	11.4	39.2	81.1	24	60.6	70.1	8.9	19.4	24.7	82.5	50.3	45.4	49.7	97.1	38.1
La	67.2	90.3	92	78.6	49.5	46.1	21.6	101.6	53.8	46	108.4	137.4	50.9	58.4	72.1	60	69.9	158.7	62	43.8	57.5
Ce	127.2	197.4	175.6	148.5	95.3	98.3	31	189.7	91	74.8	216.8	233.7	115.2	124	143	121.1	131.3	304.7	130.4	88.5	123.3
Pr	13.57	23.78	21.37	18.04	11.34	11.63	3.1	22.84	11.64	9	26.9	29.23	14.13	15.01	15.42	15.64	15.63	35.64	15.45	10.56	14.32
Nd	49.8	96.4	79.6	66.1	40.7	43.1	10.4	90.3	48.1	36.4	100.4	119.3	52.5	57.6	58.1	68.4	56.9	133.7	59.7	41.9	54.4
Sm	8.2	15.1	15.2	13.6	8	7.6	1.8	15.3	10.2	6.3	17.9	19.9	9.8	9.4	9.5	13.2	10.1	19.7	10.3	7.6	9.6
Eu	2.43	3.05	3.17	2.04	1.38	1.16	2.38	2.11	1.8	1.07	3.14	2.9	1.22	1.73	2.45	2.68	2.14	3.11	1.79	1.64	1.98
Gd	6.02	13.43	12.49	11.84	6.98	7.06	1.49	15.08	11.84	6.24	13.91	20.29	6.92	8.17	6.54	15.09	8.63	19.49	9.5	8.55	8.48
Tb	0.92	2.09	1.83	1.76	1.12	1.25	0.22	1.85	1.88	0.71	1.97	2.35	0.78	1.12	0.9	2.28	1.32	2.26	1.55	1.94	1.42
Dy	5	10.95	9.77	9.99	6.7	7.1	1.63	8.62	13.53	4.38	10.37	14.53	2.58	4.64	5.31	13.15	7.67	10.69	8.6	14.34	7.37
Ho	0.67	2.01	1.96	2.14	1.44	1.42	0.4	1.31	3	0.95	1.97	2.63	0.3	0.67	0.98	2.74	1.71	1.5	1.67	3.3	1.32
Er	1.45	5.53	5.66	6.09	4.21	4.37	1.36	3.45	8.19	2.64	5.55	7.2	0.56	1.41	2.98	8.76	5.32	3.85	4.97	10.8	3.67
Tm	0.16	0.79	0.74	0.86	0.6	0.64	0.24	0.4	1.14	0.41	0.78	1.02	0.08	0.18	0.42	1.25	0.82	0.36	0.73	1.71	0.52
Yb	1.03	4.75	4.79	5.59	3.82	3.92	1.78	2.22	6.99	2.97	4.76	6.06	0.51	1	2.8	7.9	5.29	1.95	4.68	11	3.14
Lu	0.17	0.66	0.74	0.83	0.53	0.58	0.29	0.34	0.95	0.44	0.71	0.85	0.08	0.16	0.45	1.3	0.84	0.26	0.71	1.55	0.45
Mo	1	0.6	0.6	1.3	0.8	0.6	0.5	1.3	0.8	0.3	0.7	1.1	0.3	1.3	< 1	0.6	0.7	0.8	0.8	0.4	1
Cu	30	25.1	34	22.8	13.4	17.1	18.9	33	15	9	17.6	18	3.1	30.7	19	31	41.9	27	27.5	54.6	10
Pb	< 3	4	3.8	2.6	3.6	4.9	2.2	5	4	7	2.8	10	6.5	4.1	< 3	4	3.7	6	3.7	1.6	3.6
Zn	70	114	76	73	23	21	33	61	54	106	116	98	18	65	50	40	43	76	43	39	49
Ni	28	38.4	49.1	24.7	34	29.8	35.2	43	42	32	34.6	31	10.7	42.3	28	30	31.9	39	33.1	21.1	19.6

Table 1 continued
1 lentelės tęsinys

ROCK	Charnockitic rocks of Kuršiai pluton																				
SAMPLE	Stmb-1	Slt-3	Slnt-4	Slgl-1	Tl-1	Trb-4	Trsk-73	Tbs	Vvr-1-1	Vvr-1-2	Vvr-2	Vvr-4	Vvr-5	Vvr-6	Vlc-1	Vlc-2	Vlc-3	Vd-1-2126	Vd-1-2192	Vd-1-2402	Vd-2
SiO_2	62.94	72.14	53.23	59.25	55.83	63.81	60.26	61.3	62.61	68	62.88	65.51	63.88	65.62	66	61.25	62.9	61.45	59.78	59.9	60.34
Al_2O_3	14.9	13.87	18.44	14.46	16.24	14.36	14.78	16.34	15.65	14.6	14.29	15.92	15.34	15.91	13.6	13.78	15.5	16.76	16.43	16.33	16.57
FeO	8.33	2.54	9.6	9.94	10.52	7.18	6.76	7.77	4.82	5.52	10.44	4.57	6.94	5.63	7.5	8.41	7.82	7.8	8.9	9.43	9.57
MgO	2.61	0.78	4.16	2.58	3.14	1.29	0.77	2	1.8	1.53	2.53	1.11	2.04	1.48	1.67	2.58	1.64	2.13	2.13	2.17	2.29
CaO	0.76	0.7	8.43	4.24	4.45	3.65	6.22	4.15	4.54	2.79	2.54	2.96	2.88	2.87	3.73	3.44	3.96	4.1	4.51	4.45	5.03
Na_2O	1.84	2.53	2.79	2.1	1.93	2.45	2.33	2.4	2.78	2.43	2.31	2.93	2.75	2.7	2.13	1.94	2.42	2.43	2.62	2.46	2.57
K_2O	4.65	5.44	0.75	4.05	2.18	4.45	4.53	3.78	3.51	3.69	3.44	4.09	3.63	3.84	2.94	4.66	3.84	3.96	3.3	3.08	1.63
TiO_2	0.74	0.39	0.9	1.84	1.45	1.2	1.25	1.19	1.72	0.9	0.92	0.65	1.02	0.84	0.92	1.55	1.06	0.95	1.5	1.42	1.49
P_2O_5	0.18	0.28	0.48	0.49	0.24	0.41	0.47	0.16	0.04	0.12	0.16	0.09	0.15	0.11	0.19	0.48	0.22	0.12	0.39	0.33	0.21
MnO	0.09	0.02	0.13	0.12	0.09	0.07	0.09	0.09	0.03	0.06	0.14	0.07	0.08	0.04	0.1	0.07	0.11	0.09	0.1	0.11	0.11
Cr_2O_3	0.006	0.001	0.02	0.009	0.013	0.007	0.005	0.009	0.013	0.01	0.01	0.009	0.017	0.011	0.01	0.008	0.01	0.01	0.011	0.01	0.013
Ba	981	530	458	1282	878	877	1052.3	1113	319	396.6	652.4	702.8	849.3	752.5	769	1142	1000	1383.4	936.2	1138.3	530
Sc	21	4	22	21	30	18	22	19	9	13	32	10	14	9	19	19	20	23	18	25	25
Co	20.8	3.8	27.8	24.4	22.6	13.3	10.9	18.5	14.6	13	20.7	9.8	17.1	13.7	16.5	18.1	15.3	17.3	17.5	20.8	23.8
Cs	0.6	0.6	0.2	1.6	0.9	3.1	1.1	0.3	1.4	0.4	10	0.6	19.4	0.7	0.4	1.8	0.5	0.2	0.2	0.3	0.1
Ga	21.8	18.3	25.3	23.1	29.8	25	23.3	23.1	26.5	19.1	20.8	21.3	22.4	21.7	20	20.3	19.6	22.2	22.1	23.5	28.1
Hf	7.1	6.8	8	13.1	9.5	20.8	22.4	10.5	11.1	7.7	8.2	8.4	9.1	7.8	7.3	17.9	9.5	10.5	11.8	11.2	11.7
Nb	11.7	18.3	12.5	23.8	18	28.9	35.2	20.6	35.2	13.8	10	10	15.9	12.7	12.9	30	14.1	9.8	19.6	19.8	16.7
Rb	201.5	300	17.8	164.2	72	203.2	156.3	138.5	160	127.9	191.9	147.5	305.8	166.4	107	204.2	115	121.6	88.9	102.9	45
Sn	1	2	< 1	3	< 1	3	1	1	3	2	1	1	2	3	1	3	1	1	2	2	0.9
Sr	29.3	100.8	414.4	374.2	143.2	119.2	149.8	178.6	123.7	121.1	114.2	171.9	135.8	164	132	155.8	157	208.5	192.9	207	186.6
Ta	0.5	0.6	0.6	1.2	1.1	1.9	1.9	0.9	1.9	0.7	0.6	0.7	0.9	0.6	0.8	1.8	0.9	0.4	1.2	1	1
Th	17.4	86.6	2	24.2	14.9	27.7	56.5	20.7	12.2	16.9	19.3	18	21.4	22.5	1	30.3	3.1	15.6	9	8.2	16.3
Tl	0.1	0.2	0.1	0.5	0.2	0.7	0.3	0.1	0.3	0.2	0.9	0.1	1.8	0.2	0.1	0.5	0.1	0.1	0.1	0.1	0.4
U	0.9	5.2	0.4	1.5	1.2	3.1	1.5	0.7	2.2	0.9	1.5	2.3	1.5	1.4	0.4	1.6	0.3	0.7	0.8	0.8	0.8
V	90	18	102	170	175	60	67	108	138	79	98	80	107	94	100	114	100	102	107	130	135
W	< .1	< .1	< .1	0.9	< .1	< 1	0.2	0.2	0.2	0.3	0.4	0.1	1.5	0.1	0.6	0.9	0.3	<.1	0.2	0.1	0.9
Zr	251.2	220.4	313.7	514.5	335.9	748.6	831.1	370.4	364.9	271.5	290.1	274.2	301.6	280.8	250	675.2	339	348.4	405.8	410.3	380.6
Y	65	35.7	33.8	56.2	37.7	75.9	90	55.1	13.1	24.8	35.7	29.2	23.4	20	36.1	64.6	46.1	38.3	37.7	58.5	49.3
La	60.1	100.2	52.6	104.6	68.1	129.6	255.7	78.4	45.3	43.9	51.9	49.8	53.6	55.3	40.1	119.2	42.3	67.1	58	67.8	83.3
Ce	114.5	214.6	99.7	208.6	125.2	268	554.2	162.2	95.5	91.9	108	101.9	112.4	113.2	73.9	247.6	83.6	132.9	122.5	140.5	138.9
Pr	13.75	25.94	12.51	25.43	14.67	30.62	63.31	18.42	11.17	10.79	12.92	11.83	13.26	13.39	8.61	28.21	9.75	14.85	15.05	16.74	17.48
Nd	51	91.8	48.9	101.4	53.5	119.8	231.2	68.9	41.2	39.7	48	42.7	50.5	48.9	32.8	103.9	38.4	55.9	59.3	64.9	73.5
Sm	9.9	17	9	17.2	9.4	22.7	31	10.4	6.4	6.9	8.5	7.1	8.6	8.6	6.4	16.6	7.2	8.5	11.2	11.9	13.1
Eu	1.48	1.2	2.29	3.48	2.66	3.74	3.49	2.04	1.15	1.16	1.25	1.39	1.39	1.46	1.91	2.51	1.85	2.12	1.97	2.18	2.1
Gd	9.32	11	7.8	16.83	7.98	17.87	22.9	9.07	4.4	5.85	7.79	5.49	6.54	6.82	6.31	13.73	7.06	7.53	9.3	11.1	13.47
Tb	1.5	1.56	1.04	2.14	1.08	2.73	3.66	1.6	0.64	0.98	1.42	0.88	0.99	1.03	1.04	2.36	1.35	1.35	1.53	2	1.5
Dy	9.13	7.16	5.91	10.91	5.99	16.27	17.73	9.61	2.91	4.56	7.11	4.8	4.65	4.84	5.74	12.32	7.75	7.11	7.67	10.73	9.08
Ho	2.11	1.19	1.2	1.9	1.23	3.02	3.32	1.98	0.45	0.83	1.21	0.99	0.82	0.72	1.27	2.29	1.55	1.33	1.22	2.05	1.92
Er	6.68	2.89	3.52	5.48	3.85	8.36	9.15	5.71	1.25	2.42	3.09	3.12	2.21	1.55	3.69	6.35	4.76	3.73	2.8	5.49	5.57
Tm	1.01	0.34	0.49	0.7	0.58	1.03	1.37	0.84	0.18	0.35	0.44	0.47	0.34	0.21	0.52	0.95	0.71	0.48	0.3	0.79	0.86
Yb	6.1	2	3.2	4.42	3.81	6.22	9.22	5.38	1.07	2.33	2.8	3.25	2.07	1.13	3.21	6.1	4.58	3.08	1.65	4.88	5.99
Lu	0.95	0.27	0.5	0.64	0.63	0.89	1.28	0.81	0.18	0.35	0.41	0.45	0.33	0.18	0.49	0.84	0.71	0.48	0.22	0.71	0.85
Mo	0.2	0.3	0.4	0.9	0.8	2	1.8	0.4	0.3	0.2	0.4	0.2	0.5	0.3	0.9	1.4	0.6	0.3	0.4	0.4	0.6
Cu	45.3	43.5	48.9	25	36.7	21	24.1	27.2	17.8	7.1	18	35.1	45.2	17.1	35.6	25.4	23.4	29.8	32.4	27.1	29
Pb	2.6	7.7	5.6	6	6.1	4	7.5	3.7	3.6	3.3	1.8	3.3	4.5	5.2	2.1	5.5	2.4	2.3	4.5	3.1	17
Zn	102	40	40	102	41	94	64	41	23	28	62	20	86	33	51	59	41	39	56	61	43
Ni	36	9.3	79.3	51	43.2	16	20.4	32.6	48.2	33.6	46.5	26.2	53.7	30.6	52.7	32.3	31	31.8	33.9	33	46

Table 1 continued
1 lentelės tęsinys

ROCK	Pilsotas granodiorite					Sidabravas & Ariogala plutons			Granites		
SAMPLE	Ztt-1	Klp-1	Prm-2	Grbz-1	Lgl-1	Kur-166-1	Kur-166-2	Prmd-97	Ld-179	Grz-105	Kz-65
SiO_2	64.98	62.19	61.58	58.21	62.15	57.43	60.79	63.97	66.03	67.13	67.59
Al_2O_3	14.49	13.55	14.03	14.78	13.62	16.36	16.14	14.22	14.47	13.66	14.9
FeO	7.78	8.57	7.98	9.74	8.05	10.79	9.22	7.06	5.57	6.03	5.63
MgO	1.05	1.99	2.04	2.2	1.8	1.98	1.86	1.71	1.32	1.3	1.4
CaO	4	3.91	4.17	4.83	3.77	5.21	5.09	3.98	2.07	1.94	2.69
Na_2O	2.48	2.39	2.16	2.27	2.06	3.43	3.46	2.34	2.47	2.51	2.1
K_2O	3.07	4.02	4.64	3.69	4.61	1.98	1.66	4.11	5.07	4.99	3.78
TiO_2	1.1	1.32	1.41	2.03	1.42	1.33	1.17	1.25	0.72	0.64	0.72
P_2O_5	0.43	0.55	0.52	0.75	0.61	0.44	0.33	0.37	0.23	0.16	0.22
MnO	0.11	0.09	0.1	0.12	0.1	0.17	0.16	0.09	0.05	0.08	0.08
Cr_2O_3	0.005	0.007	0.004	0.004	0.002	0.009	0.008	0.007	0.003	0.006	0.006
Ba	996	924	1232	1398	1405	765.2	374.5	1291	1282	1126	1281
Sc	23	18	19	23	19	27	25	16	15	16	16
Co	11.8	20.7	17.9	27	16.6	20.1	15.4	14.7	9.1	9.8	11.9
Cs	2.5	3.1	3.8	1.7	3.4	1	0.6	1.9	2.7	3.4	1.6
Ga	26.5	27.3	23.2	25.7	23.4	28.7	26.6	24.2	23.9	24.4	21.8
Hf	20.3	13.5	13	15	18.1	9.7	6.3	11.1	10.8	10.2	10.5
Nb	41.6	21.8	24.6	27.8	28.9	35.4	27.1	21.4	18	16.2	13
Rb	187.8	220.7	207.9	132.5	218.4	46.2	33.5	172.1	145.9	206.7	111.6
Sn	< 1	2	2	1	2	2	2	2	2	< 1	2
Sr	112.2	236.3	277	295.9	300.9	212	170.8	282.3	154.3	139.6	163.3
Ta	2.8	1.2	1.5	1.6	1.9	1	1.5	1.2	0.9	0.4	0.9
Th	23.6	50.9	39.1	24	37	2.3	2.2	19.4	15.3	29.2	25
Tl	0.3	0.5	1.1	0.5	0.5	0.1	0.1	0.3	0.3	0.4	0.4
U	2.9	3.5	4.2	2	5.4	1	0.7	1.9	2.2	2.2	1.6
V	58	145	108	139	100	114	87	113	56	52	65
W	0.5	1.3	2	1	1	0.6	0.5	< .1	0.3	< .1	< 1
Zr	769.7	492	424.5	549.6	651.9	346.8	244.7	405.8	385.3	327.3	329.1
Y	116.5	69.4	66	76.5	78.4	63.2	53.1	49.3	32	42.3	50.5
La	125.5	163.8	138.5	121.4	152.8	48.2	45.5	100.9	35.5	99.4	84.1
Ce	241.4	295.2	235.2	209.5	260.8	105.2	93.6	194.2	93.5	187.1	167.3
Pr	29.23	33.4	29.07	27.6	33.24	13.13	11.42	22.92	8.5	21.84	19.42
Nd	109.6	117.3	117.1	117.8	135	52.5	46.2	83.8	30.9	77.9	73.1
Sm	22.4	19.7	20.7	20.7	24.2	10.3	9.5	15.1	6.8	14.1	13.8
Eu	3.57	2.9	3.02	3.51	3.33	1.84	1.68	2.88	1.85	2.01	2.48
Gd	20.36	14.53	19.61	20.91	23.38	12.41	10.21	11.38	5.92	11.1	10.57
Tb	3.11	2.15	2.24	2.52	2.63	2.09	1.78	1.54	0.88	1.47	1.56
Dy	18.48	11.56	13.24	15.71	15.76	11.65	9.79	8.49	4.85	7.6	9.88
Ho	3.88	2.27	2.53	2.96	2.89	2.21	1.85	1.64	1.03	1.43	1.98
Er	11.26	6.61	6.9	7.88	7.99	6.03	5.29	4.64	3.06	3.73	6.09
Tm	1.64	0.92	0.96	1	1.09	0.81	0.76	0.62	0.44	0.5	0.85
Yb	10.48	5.67	5.85	6.37	7.05	4.75	4.86	3.88	2.87	2.94	5.42
Lu	1.61	0.83	0.8	0.86	0.96	0.7	0.72	0.58	0.45	0.44	0.84
Mo	1.7	1.4	1	1	1.8	1.8	1.4	0.5	0.2	0.3	< 1
Cu	15.7	25.5	21	37	17	35.9	31.7	15.7	12.5	8	30
Pb	3	9.9	11	4	12	2.9	2.4	5.4	2.8	4.4	< 3
Zn	68	97	88	53	113	114	42	80	72	83	40
Ni	26	36	35	32	20	39.4	29.8	21.6	16.6	28.2	25

Granitic rocks

Granitic intrusions are of irregular shape and distributed along the margins of the WLGD, hosted by migmatized supracrustals. Plutons are distinguished by negative gravity and magnetic anomalies and scarce drilling material (Figs. 1, 2).

The Kužiai pluton is characterized by one drill hole (Kužiai-65) which revealed monzogranite with garnet and cordierite well visible in hand specimen, in the amount of about 20%. The rock is coarse-grained, porphyrous, not deformed.

The Kėdainiai pluton is characterized by three drill holes – Graužai, Ledai and Krekenava. In all of them, fixed monzogranite with biotite (5–10%), small amounts of hornblende and accessory magnetite, zircon and apatite were found. Their texture is coarse-grained, porphyrous, formed by K-feldspar phenocrysts up to 10–20 mm. The structure is gneissic, with K-feldspar augen. Rocks from the Krekenava drill hole are weathered, and therefore were not analysed.

The geochemical patterns of granites fit those of charnockitic rocks. They are demonstrated on the same diagrams as charnockitic rocks and distinguished by a special symbol (Figs. 5–7). In terms of classification by Frost et al. (2001), the rocks are ferroan, alkali-calcic, subalkaline, with a high potassic content. They also show affinity to S-type granite. The Alumina Saturation Index in granite varies from 1.4 to 1.7.

REE abundance diagrams are similar to charnockitic rocks of type I (Ledai) and type II (Kužiai, Graužai) (Fig. 8, E).

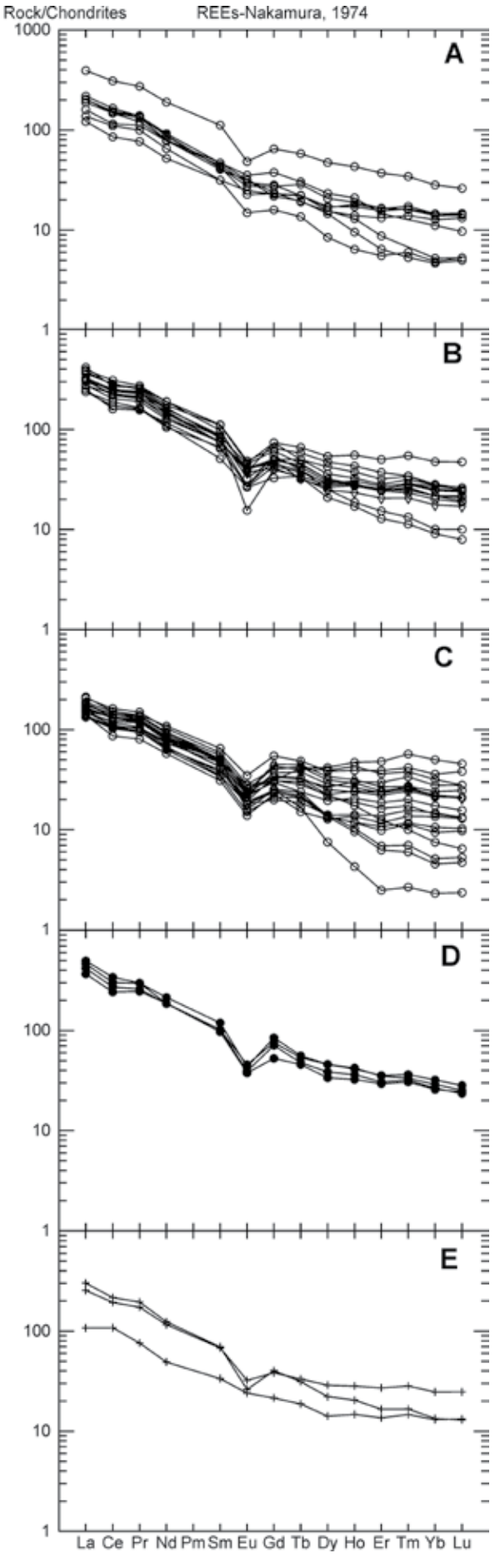

TECTONIC SETTING OF CHARNOCKITE-GRANITE SUITE

The geochemical patterns of the charnockitic and granitic suite demonstrate affinity to both A-type and S-type granites. Typically, A-type granitoids are ferroan, metaluminous, alkalic or alkali-calcic, while most of the S-type granitoids are magnesian and invariably peraluminous. Part of WLGD charnockitic-granitic rocks are ferroan, peraluminous and at the same time calc-alkalic. According to Frost et al. (2001), such rocks are rare.

Such a composition might reflect peculiarities of the magma source and tectonic environment of their formation.

Combined peraluminous and at the same time potassic magmas might be produced by melting of pelitic or semipelitic supracrustals. Charnockitic-granitic plutons are hosted by highly migmatized supracrustals with an essential part of metapelities with high alumina content. Thus, these rocks are a reliable source also for WLGD magmas. Charnockitic magmas might be derived by the melting of metapelites or might assimilate these rocks. Such a process is indicated by detrital cores observed in zircon from charnockite in the well Vydmantai-1. The identified age of the detrital cores is 2.1 and 2.45 Ga, i. e. essentially older than the age of the emplacement and crystallization of magma (1,815 Ga) (Claesson et al., 2001).

A-type granites are mainly cratonic rocks, while S-type granites are more characteristic of an orogenic environment. Thus, the formation of a charnockitic-granitic suite might occur during a transitional period from the late orogenic to cratonic environment in the thickened crust. This concept is demonstrated by diagrams in Fig. 9.

ISOTOPIC DATING

Charnockitic and granitic rocks of the WLGD where previously characterized by a single date of opdalite from the well Vydmantai 1 by the U–Pb method. The age of zircons of the magmatic phase was estimated as 1815 ± 20 Ma (Claesson et al, 2001).

The authors contributed to the dating of plutonic magmatism in the WLGD by three new dates of opdalite from the well Macuičiai-1 in the Kuršiai pluton, garnet and cordierite granite from the well Kužiai-65, and gneissic granite from the well Graužai-105. The results are listed in Table 2.

Analytical technique

U–Pb analyses were carried out at the Institute of Precambrian Geology and Geochronology in Sankt Petersburg, Russsia, using a Finnigan MAT 261 mass-spectrometer in a static and jumping (SEM) mode.

Zircons were extracted from crushed rock samples using standard heavy liquid and magnetic separation techniques. Hand-picked single zircons were ultrasonically washed in

Fig. 8. REE abundance diagrams of charnockitic and granitic rocks: *A* – group I; *B* – group II a; *C* – group II b; *D* – rocks of Pilsotas phase; *E* – granitic rocks from Kužiai, Ledai and Graužai wells

Fig. 8. Čarnokitų ir granitų RŽĖ kiekių diagramos: *A* – I grupė; *B* – Ia grupė; *C* – Ib grupė; *D* – Pilsoto fazės uolienos; *E* – granitai iš Kužių, Ledų ir Graužų gręžinių

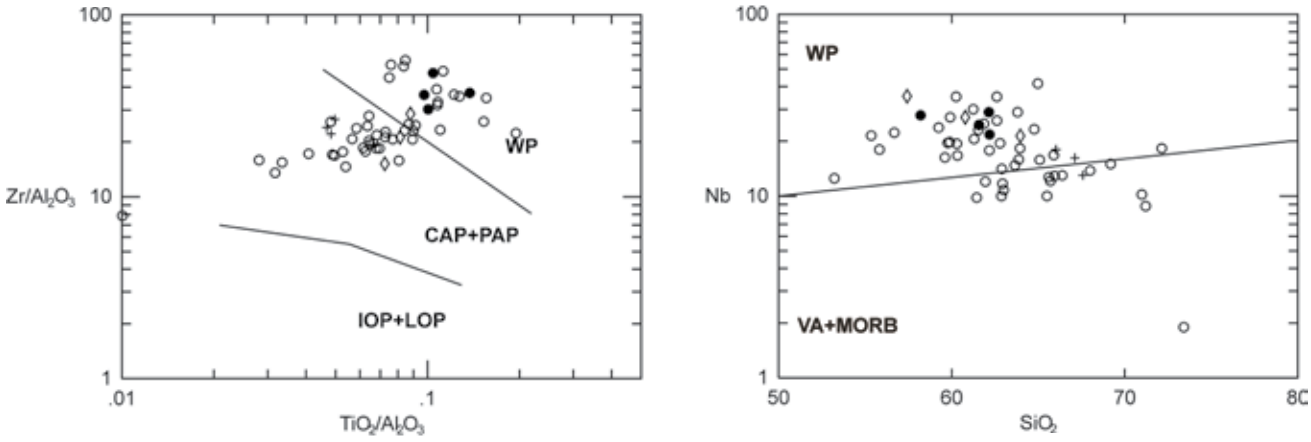

Fig. 9. Tectonic setting of WLGD charnockitic and granitic rocks on the TiO_2 / Al_2O_3 *vs* Zr / Al_2O_3 plot by Muller et al. (1992) in Carr et al., 2003 and SiO_2 *vs* Nb plot by Pearce et al., (1984). Abbreviations: IOP + LOP – field of initial and late oceanic arc magmas, CAP + PAP – continental and post-collisional arc magmas, WP – within plate magmas; VA + MORB – volcanic arcs and mid-ocean ridge magmas. Symbols as in Fig. 4

Fig. 9. VLGS čarnokitų ir granitų tektoninės padėties diagramos: TiO_2 / Al_2O_3 *vs* Zr / Al_2O_3 (pagal Muller et al., 1992; iš Carr et al., 2003); SiO_2 *vs* Nb (pagal Pearce et al., 1984). Aiškinimai: IOP + LOP – nebrandus ir vėlyvas vandenynų salų lankų magmatizmas; CAP + PAP – kontinentinių ir postkolizinių vulkaninių lankų magmatizmas; WP – kontinentinis magmatizmas; VA + MORB – vulkaninių lankų ir vandenyno vidurio gūbrių magmatizmas. Sutartiniai ženklai kaip 4 pav.

alcohol and acetone. Additionally, grains were washed in warm 1M HNO_3 and 1 : 1 HCl for 20 minutes in each acid to eliminate surface contamination. Zircon fractions consisting of 20 to 100 grains were analysed following the method of Krogh (1973). All samples were spiked with a ^{235}U–^{208}Pb mixed tracer. Total blanks were 0.01–0.05 ng Pb and 0.001 ng U. Air-abrasion followed the technique of Krogh (1982), modified by coating the abrasive walls with epoxy-impregnated diamond powder. Uncertainties, correlations of U / Pb ratios, regression lines, and concordia intercept ages were calculated employing the PBDAT and ISOPLOT programs of Ludwig (1991, 1999) and the constants recommended by the IUGS Subcommission on Geochronology (Steiger, Jäger, 1977). Correction values for the common Pb are from Stacey and Kramers (1975). All errors are reported at the 2σ level.

Sample from Macuičiai-1 (Mc) drill hole

This sample represents opdalite from the Kuršiai charnockite pluton. Zircons in this rock are subhedral, transparent and translucent, pale-pink, prismatic or short-prismatic in habit**.** Crystals are faceted mainly by prisms {100}, {110} and bipyramids {111}, {331}. On cathodoluminescence images (CL) the zircon population displays structures that are characteristic of post-crystallization disturbance: zoned inner parts are partially replaced by a secondary homogeneous phase with bright CL (Fig. 10, Mc-1, 2). Numerous grains contain an outer high-CL with virtually structure less overgrowth (Fig. 10, Mc-3, 4, 5). The grain size varies between 40 and 250 μm, and the length / width ratio is 1.2–2.5.

One unabraded and two abraded multigrain zircon fractions from sieve fractions –85 + 60 μm and –150 + 100 μm (Table 2, analyses 1–3), together with a single zircon grain extracted from CL mount using the cathodoluminescence control (CLC) method (Poller et al., 1997) (Table 2, analysis 5; Fig. 10, MC-6) were analysed. These samples demonstrate some discordance but define a regression line (MSWD = 1.3) with intercept ages at 1846 ± 12 and 1170 ± 50 Ma (Fig. 11, Mc-1). Attempting to avoid an altered zircon domain, we used preliminary acid treatment in HF + HNO_3 (Mattinson, 1994). The residue after the acid treatment is characterized by a significantly younger ^{207}Pb / ^{206}Pb age, showing a mixture of pristine magmatic and recrystallized zircon domains (overgrowths) (Table 2, analysis 4). Taking into account that a discordia was calculated for abraded zircon fractions and single zircon with a certain internal structure free from overgrowth and recrystallized zones, we consider the age of 1846 ± 12 Ma to reflect the time of emplacement of the charnockite magma.

Sample from Kužiai-65 (Kz) drill hole

This sample was taken from garnet-cordierite-bearing granite. The zircon population of this sample consists of subhedral and euhedral, transparent and pale-pink zoned grains with prismatic and long-prismatic habit (Fig. 10, Kz-1–3). Prisms {100}, {110} and bipyramids {101}, {111}, {112} represent a common morphology. Their grain size is 40 to 300 μm and the length / width ratio is 2.0–3.0. Most grains contain abundant apatite and transparent, bubble-like and opaque inclusions. Some of translucent zircons are characterized by the presence of cores and thin fractured cloudy rims (Fig. 10, Kz-4–6).

Three multigrain sieve fractions of the cleanest grains (–85 + 60 μm, –150 + 100 μm, >150 μm) were analysed (Table 2, analyses 6, 7, 8). Two of them were abraded whereby about 50% and 60% of zircon crystal volume were removed (Table 2, analyses 7, 8). The data point for the large abraded grain fraction is concordant at 1840 ± 1.9 Ma (Fig. 11). All analytical data are well aligned in the Concordia diagram and define a discord line (MSWD = 1.3) with intercept ages of 1844 ± 5 and 422 ± 30 Ma, respectively. Since the zircon morphology indicates an igneous origin, the age of 1844 ± 5 Ma is interpreted as the estimation for the time of emplacement of the granite magma.

Sample from Graužai-105 (Grz) drill hole

This sample represents gneissic granite from the Kėdainiai pluton. The sample contains subhedral, zoned, transparent or translucent, pale-pink and somewhat fractured zircons with

prismatic habit (Fig. 10, Grz-1–5). Crystals are faceted mainly by prisms {100}, {110} and bipyramids {101}, {111}. Enhancement of CL emission ("bleaching") and concurrent fading of zonation could indicate a disturbance of the U–Pb system. Several grains contain core relics as well as highly luminescence overgrowths (Fig. 10, Grz-6). The grain size is 30 to 400 μm and the length / width ratio is 2.5–4.7.

Three abraded zircon fractions where analysed (Table 2, analyses 9, 10, 12) and one fraction (>150 μm) was subjected to a preliminary acid treatment (Table 2, analysis 11). The data point for analysis is concordant and yielded a ^{207}Pb / ^{206}Pb age of 1836 ± 2.0 Ma and a calculated concordia age of 1832 ± 5 Ma (Table 2, Fig. 11). The regression line defined by three analyses of zircon from the sieve fraction >150 μm (MSWD = 1.07) intersects the concordia at 1837 ± 6 Ma and 170 ± 170 Ma, respectively. Abraded zircons from fraction –80 + 60 μm (Table 2, analysis 12) are characterized by a somewhat older ^{207}Pb / ^{206}Pb age (1848 ± 2.0 Ma) indicating a possible inheritance. Based on the morphology suggesting a magmatic origin for zircons from this sample, the upper intercept age of 1837 ± 6 Ma is interpreted to most closely approximate the intrusion of granite.

All available dating results suggest formation of the main part of the Kuršiai charnockitic batholith and adjacent granitic plutons during the 1846–1837 Ma time span, while particular phases and plutons are younger – about 1815 Ma.

CONCLUSIONS

A number of charnockitic and granitic intrusive plutons have been revealed in the crystalline crust in West Lithuania. The largest Kuršiai polyphase batholith occupies an area of 140 × 80 km and is composed of various charnockitic rocks – charnockite, opdalite, mangerite and enderbite.

The petrographic and mineralogical features of the rocks indicate a primary magmatic origin of hypersthene, quartz and K-feldspar paragenesis in charnockitic rocks.

Both charnockitic and granitic rocks are predominantly ferroan, alkali-calcic and calc-alkalic, subalkaline, high potassic to shoshonitic. The geochemical patterns of the rocks reveal affinity both to S- and A-type granite and suggest the formation of plutons during the transitional period from the orogenic to the cratonic tectonic environment.

Table 2. **U–Pb isotopic data for conventional and single grain analyses of zircon**
2 lentelė. **Cirkono standartinių ir atskirų grūdų U–Pb izotopinių tyrimų duomenys**

[1]	Sieve fraction, μm	Fraction weight, mg	Concentrations ppm		206Pb / 204Pba	Isotopic ratios corrected for blank and common Pbb			Rhoc	Age, Ma		
			Pb	U		207Pb / 206Pb	208Pb / 206Pb	207Pb / 235U	206Pb / 238U	207Pb / 235U	206Pb / 238U	207Pb / 206Pb
	Sample Mc-1											
1	–85 + 60	0.44	96.6	344	5366	0.1039 ± 1	0.0455 ± 1	4.0429 ± 81	0.2821 ± 6	0.96	1643 ± 3	1602 ± 3	1696 ± 0.7
2	–150 + 100, A40%	0.26	64.0	200	3131	0.1104 ± 1	0.0561 ± 1	4.7913 ± 96	0.3149 ± 6	0.94	1783 ± 4	1765 ± 4	1805 ± 0.8
3	–150 + 100, A70%, 10 gr.	–	U/Pb*	=3.1	1987	0.1104 ± 2	0.0626 ± 1	4.8408 ± 136	0.3181 ± 6	0.62	1792 ± 5	1781 ± 4	1805 ± 4.0
4	–150 + 100, acid treatment	–	U/Pb*	=3.4	8019	0.0998 ± 1	0.1495 ± 1	3.8051 ± 76	0.2766 ± 6	0.95	1594 ± 3	1574 ± 3	1620 ± 0.8
5	1 single gr.	–	U/Pb*	=3.2	1520	0.1096 ± 2	0.0325 ± 1	4.7103 ± 250	0.3118 ± 16	0.96	1769 ± 9	1750 ± 9	1792 ± 3
	Sample Kz-65											
6	–85 + 60	0.80	75.7	236	9957	0.1118 ± 1	0.0776 ± 1	4.813 ± 10	0.3122 ± 6	0.97	1787 ± 4	1751 ± 4	1829 ± 0.6
7	–150 + 100, A50%	0.40	44.7	134	4907	0.1125 ± 1	0.0695 ± 1	5.044 ± 10	0.3252 ± 7	0.95	1827 ± 4	1815 ± 4	1840 ± 0.8
8	>150, A 60%	0.42	22.6	65.6	1180	0.1124 ± 1	0.0613 ± 1	5.112 ± 10	0.3296 ± 7	0.89	1838 ± 4	1837 ± 4	1840 ± 1.9
	Sample Grz-105											
9	>150 A70%	0.26	16.9	52.0	1512	0.1121 ± 2	0.1023 ± 1	4.7403 ± 95	0.3067 ± 6	0.68	1774 ± 4	1725 ± 3	1833 ± 2.5
10	>150 A20%	0.41	43.7	136	3199	0.1118 ± 1	0.0937 ± 1	4.7508 ± 95	0.3081 ± 6	0.93	1776 ± 4	1731 ± 3	1830 ± 0.9
11	>150, acid treatment	–	U/Pb*	=2.8	981	0.1123 ± 1	0.1239 ± 1	5.0736 ± 101	0.3278 ± 7	0.76	1832 ± 4	1828 ± 4	1836 ± 2.0
12	–80 + 60, A30%	0.44	11.6	35.7	2276	0.1130 ± 1	0.0989 ± 1	4.8713 ± 122	0.3126 ± 8	0.91	1797 ± 4	1754 ± 4	1848 ± 2.0

Notes: [a] measured ratio; [b] uncertainties (95% confidence level) refer to last digits of corresponding ratios; [c] correlation coefficients of ^{207}Pb / ^{235}U vs. ^{206}Pb / ^{238}U ratios; U / Pb* – U / Pb ratios for unweighted grains were determined using the ^{208}Pb / ^{235}U spike solutions; A 50% – amount of zircon removed during air abrasion; 2 single gr. – amount of zircon grains analysed.

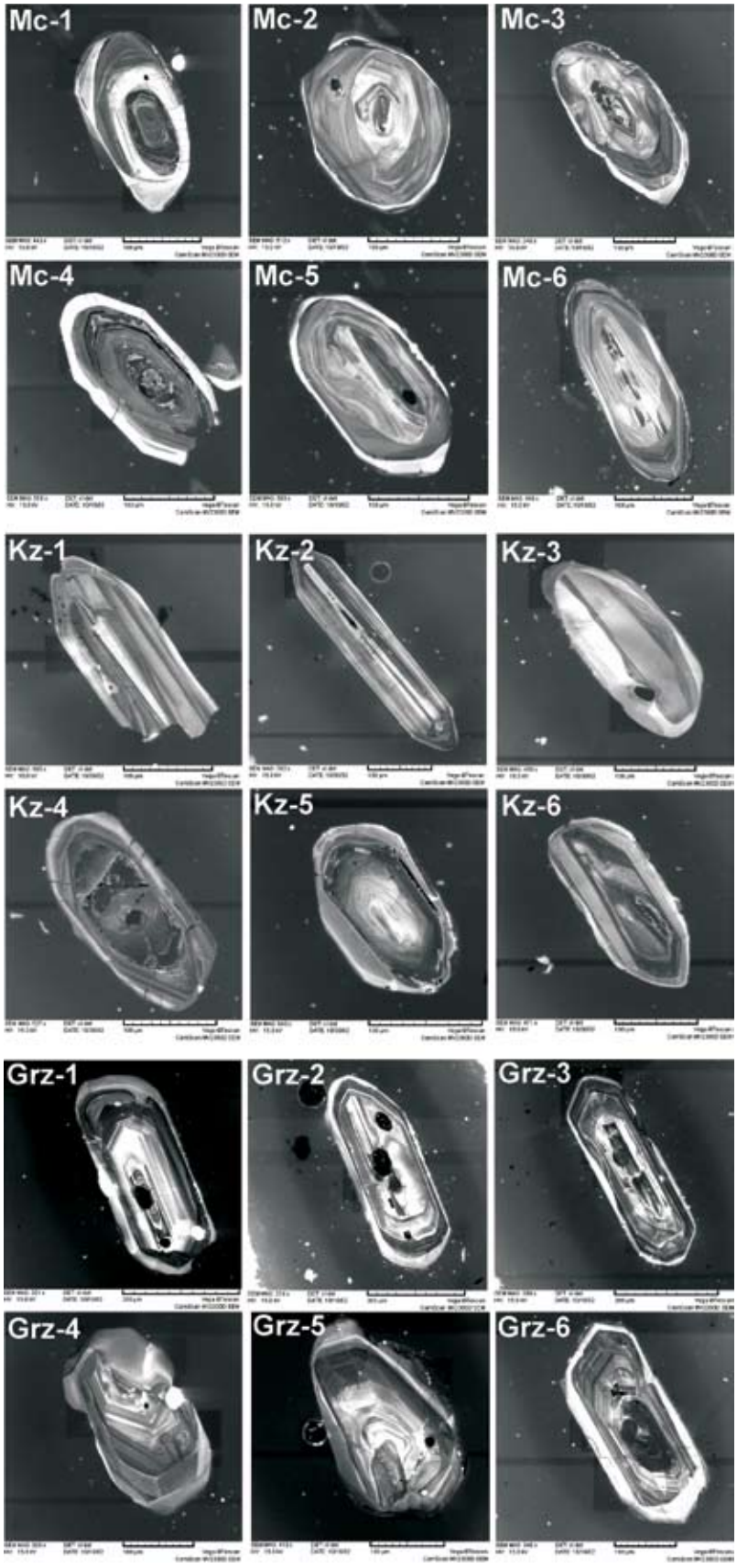

Fig. 10. Cathodoluminescence images of zircons from samples dated by U–Pb method: Mc – drill-hole Macuičiai-1, Kz – drill-hole Kužiai-65, Grz – drill-hole Graužai-105

Fig. 10. Cirkono, datuoto U–Pb metodu, katodoliuminescencinės nuotraukos: Mc – Macuičių-1 gręžinys; Kz – Kužių-65 gręžinys; Grz – Graužų-105 gręžinys

Extensive charnockitic and coeval granitic magmatism in the WLGD took place between 1850–1815 Ma, manifesting a certain magmatic phase in the formation of the continental crust in this part of the Svecofennian domain.

ACKNOWLEDGEMENTS

This work was started in the course of compilation of the geological map of the crystalline basement of Lithuania, financed by the Geological Survey of Lithuania. Later studies were continued as part of the VISBY program project "Major weakness zones in the lithosphere of western Baltica" supported by the Lithuanian Science and Studies Foundation, and the Special Foundation of Vilnius University. The authors wish to acknowledge all these institutions for their essential contributions.

References

1. Barker F. 1979. Trondhjemite; definition, environment and hypotheses of origin. In: Barker F. (ed.). *Trondhjemites, dacites, and related rocks*. 1–12.
2. Bogdanova S., Gorbatchev R., Grad M., Guterch A., Janik T., Kozlovskaja E., Motuza G., Skridlaite G., Starostenko V., Taran L. & EUROBRIDGE and POLONAISE Working Groups. 2006. EUROBRIDGE: New insight into the geodynamic evolution of the East European Craton. European Lithosphere Geodynamics. *Geological Society London Memoirs*. 599–625.
3. Carr P. F., Fergusson C. L., Pemberton J. W., Colquhoun G. P., Murray S. I., Watkins J. 2003. Late Ordovician island-arc volcanic rocks, northern Capertee Zone, Lachlan Fold Belt, New South Wales. *Australian Journal of Earth Sciences*. ***50.*** 319–330.
4. Chappel B. W., White J. R. 2001. Two Contrasting Granite Types: 25 years later. *Australian Journal of Earth Sciences*. ***48.*** 489–499.
5. Claesson S., Bogdanova S., Bibikova E. V., Gorbatschev R. 2001. Isotopic Evidence for Palaeoproterozoic Accreation in the Basement of the East European Craton. *Tectonophysics*. ***339.*** 1–18.
6. Dörr W., Belka Z., Marheine D., Schastok J., Valverde Vaquero P.,

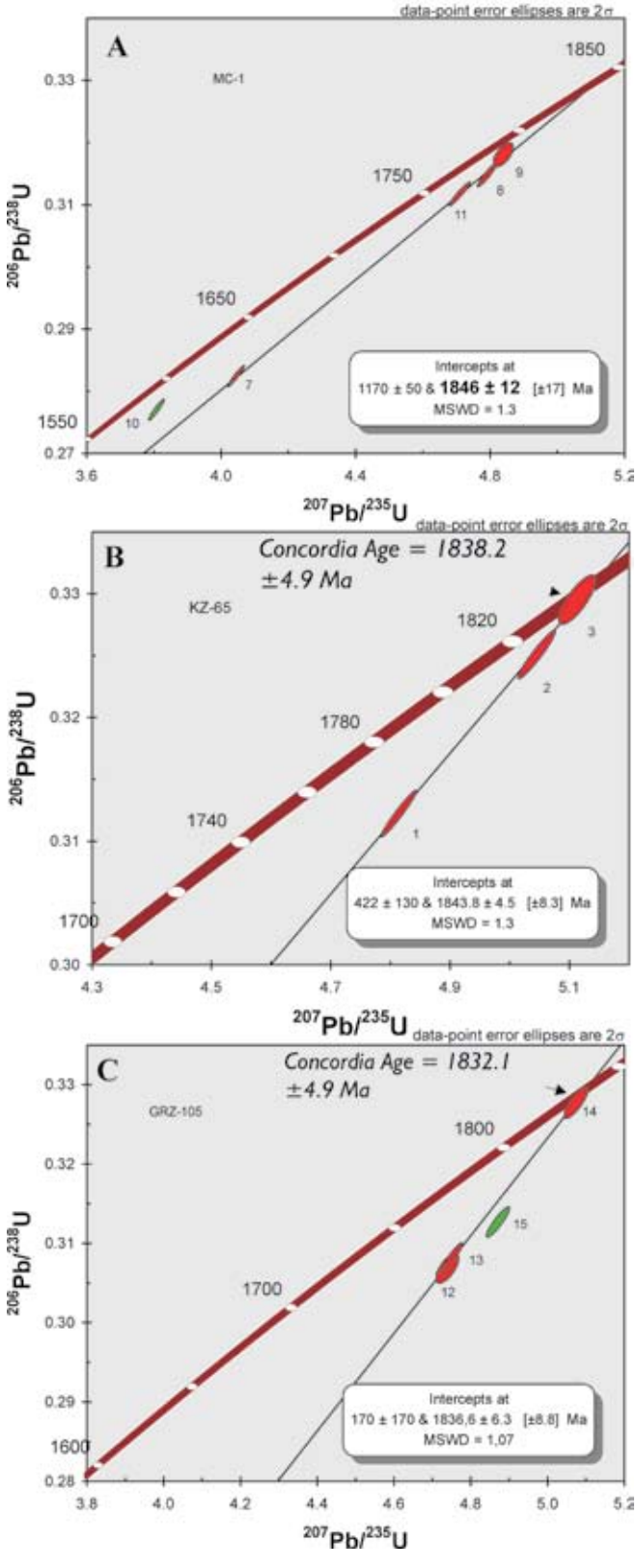

Fig. 11. U–Pb concordia diagrams for opdalite from Macuičiai-1 well (MC-1), garnet and cordierite granite from Kužiai-65 well (KZ-65), biotite granite from Graužai-105 well (GRZ-105). See Fig. 1 for sample localities and Table 2 for analytical data

Fig. 11. U–Pb konkordijos diagramos: Mc-1 – opdalitas iš Macuičių-1 gręžinio; KZ-65 – granatinis ir kordieritinis granitas iš Kužių-65 gręžinio; GRZ-105 – biotitinis granitas iš Graužų-105 gręžinio. Gręžinių padėtį žemėlapyje žr. 1 pav.; tyrimų duomenis žr. 2 lentelėje

Wiszniewska J. 2002. U–Pb and Ar–Ar geochronology of anorogenic granite magmatism of the Mazury complex NE Poland. *Precambrian Research. Special issue*. Ed. T. Rämo. ***119.*** 101–102.

7. EUROBRIDGE'95 seismic working group, Yliniemi J. et al. 2001. EUROBRIDGE'95 Deep Seismic Profiling within the East European Craton. *Tectonophysics*. ***339.*** 153–175.
8. Frost B. R., Barnes C. G., Collins W. J., Arculus R. J., Ellis D. J., Frost C. D. 2001. A geochemical classification for Granitic Rocks. *Journal of Petrology*. ***42***(*11*). 2033–2048.
9. Giese R. 1998. Eine zweidimensionale Interpretation der Geschwindigkeitsstruktur der Erdkruste des südwestlichen Teils der Osteuropäischen Plattform (Project EUROBRIDGE). *Scientific Technical Report STR98/16*. Potsdam. 190 p.
10. Krogh T. E. 1973. A low-contamination method for hydrothermal decomposition of zircon and extraction of U and Pb for isotopic age determination. *Geochimica et Cosmochimica Acta*. ***37.*** 485–494.
11. Krogh T. E. 1982. Improved accuracy of U–Pb zircon ages by creation of more concordant systems using an air abrasion technique. *Geochimica et Cosmochimica Acta*. ***46.*** 637–649.
12. Lietuvos geologija. 1994. (Geology of Lithuania in Lithuanian, abstract in English). 448 p.
13. Ludwig K. R. 1991. PbDat for MS-DOS, version 1.21. *U. S. Geological Survey Open-File Report 88–542*. 35 p.
14. Ludwig K. R. 1999. ISOPLOT/Ex. version 2.06. A geochronological toolkit for Microsoft Excel. *Berkley Geochronology Center Sp. Publ.* ***1a.*** 49 p.
15. Maniar P. D., Piccoli P. M. 1989. Tectonic discrimination of granitoids. *Geol. Soc. America Bull.* ***101***. 635–643.
16. Mattinson J. M. 1994. A study of complex discordance in zircons using step-wise dissolution techniques. *Contrib. Mineral. Petrol.* ***116***. 117–129.
17. Motuza G. 2005a. Structure and Evolution of the Crystalline Crust. Evolution of Geological Environment in Lithuania. CD. 9–18.
18. Motuza G. 2005b. Structure and formation of the crystalline crust in Lithuania. *Polskie Towarzystwo Mineralogiczne – Prace specjalne. Mineralogical Society of Poland – Special Papers*. ***26***. 69–79.
19. Motuza G., Vėjelytė I. 2005. Telšių tektoninių deformacijų zonos petrologinis apibūdinimas. The petrologic characteristic of the Telšiai deformation zone (in Lithuanian, abstract in English). *Geologija*. ***49.*** 1–9.
20. Motuza G., Čečys A., Salnikova J., Kotov A. 2006. The Žemaičių Naumiestis granitoids: new evidences for Mesoproterozoic magmatism in western Lithuania: *GFF*. ***128.*** 243–254.
21. Muller D., Rock N. M. S., Groves D. I. 1992. Geochemical discrimination between shoshonitic and potassic volcanic rocks in different tectonic settings: a pilot study. *Mineralogy and Petrology*. ***46.*** 259–289.
22. Pearce J., Harris N. B. W., Tindle A. G. 1984. Trace Element Discrimination Diagrams for the Tectonic Interpretation of Granitic Rocks. *Journal of Petrology*. ***25.*** 956–983.

23. Peccerillo R, Taylor S. R. 1976. Geochemistry of Eocene calc-alkaline volcanic rocks from Kastamonu area, northern Turkey. *Contrib. Mineral. Petrol.* ***58***. 63–81.
24. Poller U., Liebetrau V., Todt W. 1997. U–Pb single-zircon dating under cathodoluminescence control (CLC-method): application to polymetamorphic orthogneisses. *Chemical Geology.* ***139***. 287–297.
25. Rajesh H. M., Santosh M. 2004. Charnockitic magmatism in Southern India. *Proc. Indian Acad. Sci.* (*Earth Planet. Sci*). ***113***(*4*). 565–585.
26. Rämö O. T., Huhma H., Kirs J. 1996. Radiogenic Isotopes of the Estonian and Latvian Rapakivi Granite Suite: New Data from the Concealed Precambrian of the East European Craton. *Precambrian Research*. ***79.*** 209–226.
27. Skridlaite G., Baginski B., Whitehouse M. 2007a. New evidence for c. 1.7–1.6 Ga metamorphism in western East European Craton from zircon and monazite study. *Geophysical Research Abstracts*. ***9***.
28. Skridlaitė G., Whitehouse M., Rimša A. 2007b. Evidence for a pulse of 1.45 Ga anorthosite-mangerite-charnockite-granite (AMCG) plutons in Lithuania: implication for Mesoproterozoic evolution of the East European Craton. *Terra Nova*. ***19.*** 294–301.
29. Stacey J. S., Kramers I. D. 1975. Approximation of terrestrial lead isotope evolution by a two-stage model. *Earth Planet. Sci. Lett.* ***26***(*2*). 207–221.
30. Steiger R. H., Jäger E. 1976. Subcomission of Geochronology: convention of the use of decay constants in geo- and cosmochronology. *Earth Planet. Sci. Lett*. ***36***(*2*). 359–362.
31. Stirpeika A. 1999. Tectonic Evolution of the Baltic Syneclise and Local Structures in the South Baltic Region with Respect to their Petroleum Potential. 112 p.
32. Sundblad K., Mansfeld J., Motuza G., Ahl M., Claesson S.1994. Geology, Geochemistry, and Age of a Cu–Mo Bearing Granite at Kabeliai, Southern Lithuania. *Mineral Petrol*. ***50.*** 43–57.
33. Whalen J. B., Currie K. L., Chappell B. W. 1987. A-type Granites: Geochemical Characteristics, Discrimination and Petrogenesis. *Contrib. Mineral Petrol*. ***95***. 407–419.

Gediminas Motuza, Vykintas Motuza, Jekaterina Salnikova, Aleksandr Kotov

PLATAUS MASTO ČARNOKITINIS-GRANITINIS MAGMATIZMAS VAKARŲ LIETUVOS KRISTALINĖJE PLUTOJE

S a n t r a u k a

Sudarant Lietuvos kristalinio pamato žemėlapį, Vakarų Lietuvos granulitų srityje (VLGS) buvo nustatyta keletas čarnokitoidų ir granitoidų intrūzinių kūnų. Didžiausias iš jų – Kuršių batolitas – užima maždaug 140 × 80 km plotą. Jis išskirtas remiantis neigiamomis gravitacinio ir magnetinio lauko anomalijomis ir maždaug 86-ių gręžinių kerno medžiaga. Čarnokitoidų intruzijas sudaro vidutinės ir rūgščios sudėties uolienos – čarnokitas, enderbitas, mangeritas, opdalitas. Uolienų geocheminės ypatybės apibūdintos remiantis 53-iomis analizėmis, gautomis ICP-MS ir ES metodais. Nustatytos uolienų geocheminės ypatybės yra būdingos tiek A, tiek S tipo granitoidams. Uolienos yra geležingos, šarminės-kalcinės ir kalcinės-šarminės, nuo kalingų iki šošonitinių, didelė jų dalis yra aliumingos ir turi kitus S tipo granitoidų požymius. Keturios U–Pb ID-TIMS cirkono datos rodo, kad čarnokitų ir granitoidų intruzijos susidarė tarp 1,85–1,815 mlrd. metų, greičiausiai pereinamuoju laikotarpiu nuo orogeninės iki kratoninės plutos susidarymo stadijos.

Гедиминас Мотуза, Викинтас Мотуза, Екатерина Сальникова, Александр Котов

ПРОЯВЛЕНИЕ ШИРОКОМАСШТАБНОГО ЧАРНОКИТОВОГО И ГРАНИТОВОГО МАГМАТИЗМА В КРИСТАЛЛИЧЕСКОЙ КОРЕ ЗАПАДНОЙ ЛИТВЫ

Р е з ю м е

В ходе составления геологической карты кристаллического фундамента Литвы было выявлено несколько интрузивных тел чарнокитового и гранитового состава в пределах Западно-Литовской гранулитовой области. Самый крупный из них – батолит Куршю занимает площадь примерно 140 × 80 км. Он выявлен на основе отрицательных аномалий гравитационного и магнитного полей и кернового материала 86 скважин. Чарнокитовые плутоны состоят из пород среднего и кислого состава – чарнокита, эндербита, опдалита, мангерита. Геохимические их особенности охарактеризованы 53 анализами, выполненными методами ICP-MS и ES. Выявлены геохимические признаки, характерные для гранитойдов как типа A, так и типа S. Породы являются железистыми, известково-щёлочными и щёлочно-известковыми, высококалиевыми до шошонитовых. В то же время многие породы являются высокоглиноземистыми и обладают другими признаками гранитойдов типа S. Четыре датировки методом U–Pb ID-TIMS по цирконам показывают, что интрузии чарнокитов и гранитов образовались между 1,85–1,815 млрд. лет, предположительно в переходный период от орогенной к кратонной стадии корообразования.